

## Numerical Modeling of Heat Transfer in a Full Scale Industry Furnace

Jørgen Furu<sup>1</sup>, Andreas Buchholz<sup>2</sup>

<sup>1</sup>Hydro Aluminium Sunndal, Research and Technology Development, P. box. 219, 6601 Sunndalsøra, Norway

<sup>2</sup>Hydro Aluminium Rolled Products GmbH, R&D, P.O. Box 2468, D-53014 Bonn, Germany

Keywords: aluminium, heat transfer, CFD, modeling, reverberatory industry furnace, casthouse, aluminium, oxy-fuel, combustion

### Abstract

A numerical model using the commercial software ANSYS Fluent was previously established for one of Hydro Aluminium's furnaces at the Rolling Mill plant in Karmøy, Norway, to analyze heat transfer conditions in the 35-ton casthouse furnace. The model was extended to evaluate a low temperature oxy-fuel burner technology different from the burners currently used today. It incorporates gas flow, chemical reactions, conduction, convection and radiation along with latent heat release. A steady state model with a heat sink was used to attain representative furnace conditions before switching to transient calculation. The focus of this work is to look at the influence of possible turbulence models and combustion models for this setup. Results confirm clear differences between the applied turbulence models and combustion models.

### Introduction

The background for the initial analysis was the necessity to reduce costs in the industry. Rising energy prices have put pressure on finding ways to reduce the energy consumption for casthouse furnaces. Limited investment budgets have resulted in a need to optimize present operation.

Hydro Aluminium R&D has previously developed a furnace model describing heat flow, including heat transfer mechanisms, to analyze possible options to improve energy efficiency in a furnace at the rolling mill plant in Karmøy, Norway [1]. The batch furnace has a nominal capacity of 35t, adding around 20t of cold metal and 12t of potroom metal in addition to the heel from the last charge. Two cold air burners with nominal power of 2.5 MW and 1.0 MW constitute the heat source in the furnace.

A separate model was later established using Low Temperature Oxy-Fuel (LTOF) burner technology for the same furnace [2]. Several factors as burner input, furnace wall emissivity, metal emissivity and dross layer were investigated in addition to a comparison of the burner technology in this effort. The results show that the LTOF burners provide a heating and melting rate considerably higher than the current setup in production today. The combined burner input of 2.3 MW or 3.0 MW for the LTOF burner's results in overheating of the furnace which can be seen in the flue gas temperatures in Figure 1. An adjustment of the burner input to 50% of the original input for the air-fuel burners gave comparable furnace temperatures with still increased heat transfer to the metal load as can be seen in Figure 2.

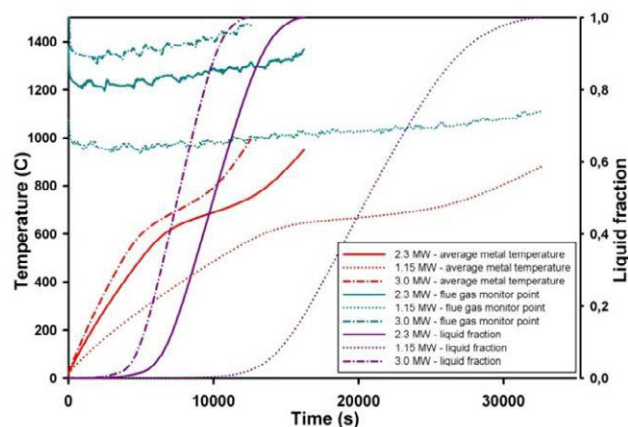


Figure 1: Melt pool configuration comparison of melting cycle using 1.15 MW, 2.3 MW and 3.0 MW of total power input for LTOF burners [2].

In this work the focus is looking at the differences in two equation turbulence models and 2-step combustion models for the furnace results. In order to limit calculation costs more comprehensive models are omitted. There are some limitations in the model such as a static metal geometry during melting and the neglect of metal oxidation. Experimental results have also shown over prediction of temperatures in the numerical model [3]. In the pilot scale furnace this indicated a burner input of around 92% in the numerical model to match the measured temperatures. The heat flux into the metal is dominated by radiation even more for the LTOF burners than the air-burners due to the difference in gas composition.

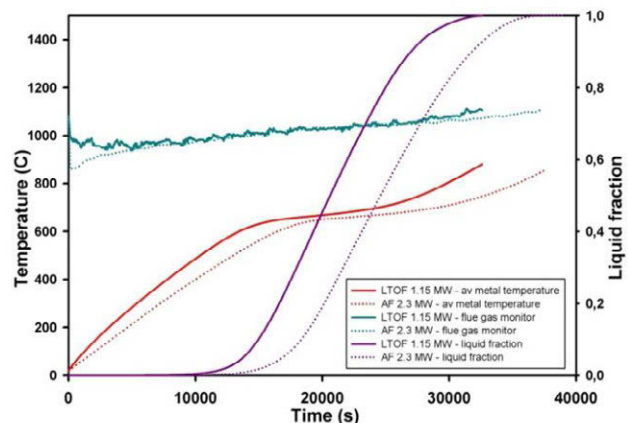


Figure 2: Furnace evaluation for melt pool configuration for 1.15 MW LTOF burner input and 2.3 MW air-fuel burner input [2].

### Numerical model

The commercial software ANSYS FLUENT 14.0 was used for the furnace covering the physical phenomena:

1. gas flow
2. combustion (chemical reaction)
3. heat conduction and advection in the gas
4. heat conduction in the metal and the walls
5. radiation
6. heat of fusion.

### Turbulence models

Gas flow is modeled using 2-equation Reynolds Averaged Navier Stokes (RANS) equations for incompressible turbulent flow. Differences between turbulence models can influence the furnace conditions and heat transfer to the metal. The turbulence models k-epsilon, Re-Normalization Group (RNG) k-epsilon, k-omega and shear stress transport (SST) k-omega are evaluated in this report.

The advantage of the k-epsilon model is its robustness and validity for fully turbulent flows and that it is computationally cheap. It performs less well for complex flows with severe pressure gradients.

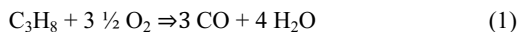
The RNG k-epsilon model has an enhanced treatment of motion in the smaller scales due to that the eddy viscosity is calculated from more than one single turbulence length scale. This can be beneficial since parts of the furnace space have a range of flow velocities. However convergence ability might be reduced with the extra term in the epsilon equation and the accuracy depends on appropriate treatment in the near-wall region.

The k-omega model from Wilcox [4] enables good performance near wall boundary layers in flows and low-Reynolds number flows along with better numerical stability. Separation is typically over predicted and early, and it requires fine mesh resolution near the walls.

The SST version of the k-omega model combines near wall treatment of k-omega with the k-epsilon away from the wall using a blending function. The same requirement for the mesh resolution near the wall is needed and involves a dependency on the wall distance.

### Combustion models

Combustion and chemical reactions are modeled using a 2-step reaction scheme:



The choice of energy source depends on availability and in some regions natural gas would be more usual. Transport equations are solved for each chemical component. The Eddy Dissipation model gives the mean reaction rate for the species based on the turbulent mixing rate. It assumes that chemical reactions occur much faster than turbulence mixes reactants. When this is not the case, the Finite-rate/Eddy Dissipation model chooses the smaller of the mixing rate and the Arrhenius rate. The Eddy Dissipation Concept is an extension of the Eddy Dissipation model where it assumes that the reactions occur in the small turbulent scales, determined by detailed Arrhenius chemical kinetics.

The combustion models using Finite-rate/Eddy Dissipation, Eddy Dissipation and Eddy Dissipation Concept are solved and compared.

### Radiation

Radiation heat transfer is modeled using Discrete Ordinates radiation model using 3 angles discretization in each quadrant and a pixilation of 5, i.e. number of pixel for each control angle. Absorption effects of the gas are included in this model in addition to radiation between surfaces.

### Melting

Phase change and latent heat in the metal is covered by a source based method of the Enthalpy formulation [5] since the built-in phase change model is not compatible with the combustion model. A limitation of the model is that the metal has a static geometry with no actual phase change but rather covers this by adding latent heat release using a source based formulation during the melting process [5]. To compensate this limitation, two metal arrangements covering different aspects of the melting process were previously applied. The first configuration is of 27 stacked ingots representing the geometry during the first part of the melting cycle. The second metal configuration is of a melt pool covering the later part of the melting cycle. The difference in heat transfer to the metal between the configurations can be seen in Figure 5. In this work no further treatment is done for the ingot arrangement as results are assumed to apply equally for the two configurations.

### **Furnace layout**

The furnace geometry was simplified based on CAD-drawings from the supplier of the furnace along with appropriate simplifications of the burner geometry. The refractory was modeled as thick walls. The original burner input for the burners of a total of 2.3 MW is adjusted to 1.15 MW for the oxy-fuel arrangement applied here. This was done to match the melting of metal in a comparable cycle to the air-fuel burners [1].

Figure 3 and Figure 4 shows the two basic metals arrangement. Tetrahedral cells were dominating the mesh geometry and later converted into polyhedral cells were feasible. The total mesh size is 2.4 million tetrahedral cells in the ingot arrangement in Figure 3. The total mesh size for the melt pool configuration in was 2.5 million tetrahedral cells which was converted into 0.4 million polyhedral cells. A comparison of the differences in metal and furnace temperatures is found in Figure 5 and results for this configuration can be reviewed based on these differences. In addition to the basic cases, cases with different burner input were previously investigated along with furnace refractory emissivity, metal emissivity and introduction of a simplified dross layer. These cases can be further reviewed elsewhere [2].

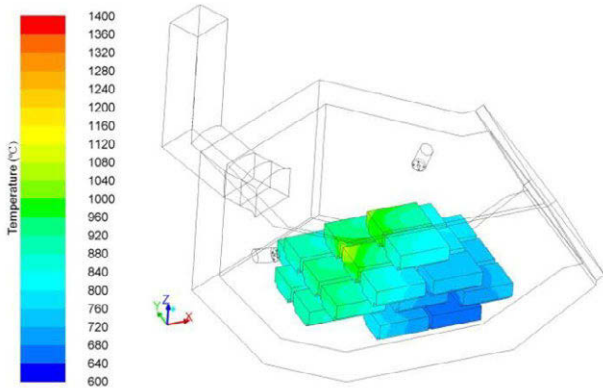


Figure 3: Metal temperature (°C) in steady state solution for industry furnace with 20 ton ingot arrangement.

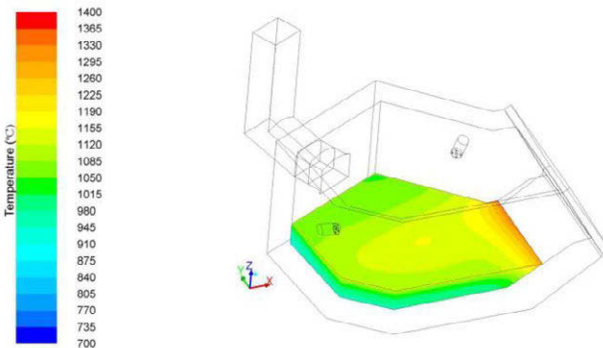


Figure 4: Metal temperature (°C) in steady state solution for industry furnace with 20 ton melt pool configuration.

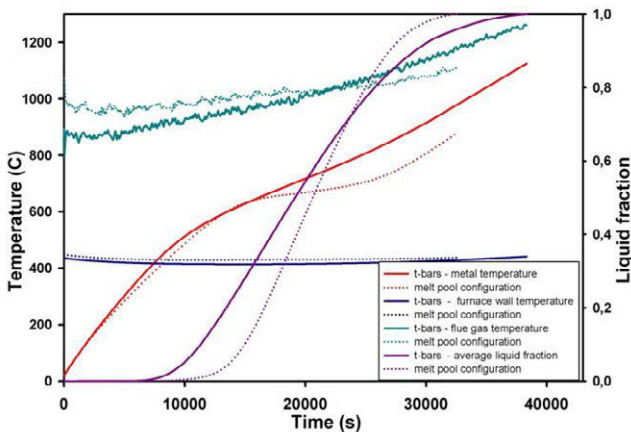


Figure 5: Difference in furnace temperatures with two metal configurations [2].

### Steady state cases

To avoid the implications of modeling the complete ignition process, steady state calculations of the two metal configurations are performed to provide a stable flame configuration for the start of the transient calculations. A heat sink is introduced in the metal during the steady state calculations to prevent the model from overheating:

$$\alpha_{\text{heatsink}} = \frac{C_p(T_{\text{end}} - T_{\text{init}}) + L}{(T_{\text{furnace}} - T_{\text{average metal}})t_m} \quad (3)$$

The heat sink allows a chosen furnace temperature,  $T_{\text{furnace}}$ , and metal temperatures,  $T_{\text{average metal}}$ , to be attained along with the desired melting time,  $t_m$ .

A melting time of 4 hours along with a furnace temperature of 1000°C and a metal temperature of 500 °C is found appropriate for the strength of the heat sink which is dynamically adjusted to the furnace condition.

### Transient calculations

The results for the transient calculations are based on the steady state solutions where the temperature in the aluminium metal is reinitialized to 20°C. The heat sink is then removed while the latent heat term is activated. The material properties used for the furnace cases are be found in Table 1.

Table 1: Material properties

Parameter	Value	Unit
Refractory emissivity, $\epsilon$	0.6	
Refractory density, $\rho$	2320	Kg/m <sup>3</sup>
Refractory specific heat capacity, $C_p$	1138	J/(kg K)
Refractory conductivity, $k$	0.5	W/(m K)
Aluminium emissivity, $\epsilon$	0.3	
Aluminium density, $\rho$	2350	Kg/m <sup>3</sup>
Aluminium specific heat capacity, $C_p$	1080	J/(kg K)
Aluminium conductivity, $k$	200	W/(m K)

The boundary conditions for the furnace outside walls to the surroundings are set at a convection boundary condition of 300 W/m<sup>2</sup>. This is a simplification of the total heat boundary condition approximating the sum of convection and radiation heat transfer.

Except from changes in properties explicitly described all other conditions are set identical for all investigated cases.

### Turbulence models

The results in Figure 6 shows that the k-omega and the SST k-omega model have smoother changes in the chamber temperature than the k-epsilon and the RNG k-epsilon models, which displays more rapid fluctuations. All turbulence models do however follow the same temperature evolution for the chamber temperature and it is noted that the presumed instabilities for the two latter models seem to decrease with time. The reason for the fluctuations in the k-epsilon and RNG k-epsilon model might be due to flow regions with large gradients between pressure gradient and insufficient boundary layer treatment. The average liquid fraction for the metal melt pool configuration correspond closely for all models, which indicates that the differences between the models might not have crucial significance for the heat transfer to the metal.

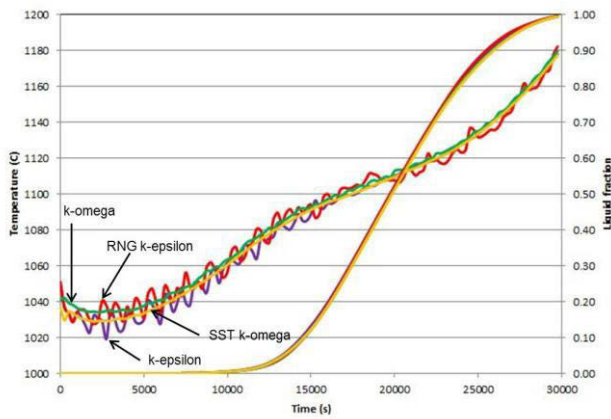


**Figure 6: Average furnace chamber temperature and liquid fraction, for melt pool configuration, for turbulence models k-epsilon, RNG k-epsilon, k-omega and k-omega-SST.**

The average flue gas temperature, in Figure 7, displays the same behavior of oscillating temperatures for the k-epsilon and the RNG k-epsilon model compared to the SST k-omega and the k-omega turbulence models. The flue gas temperature for the SST k-omega model is moreover slightly less oscillating in comparison to the k-omega model. This might indicate that there is a need for a careful treatment of the flow both near the boundary layer and in free stream conditions.

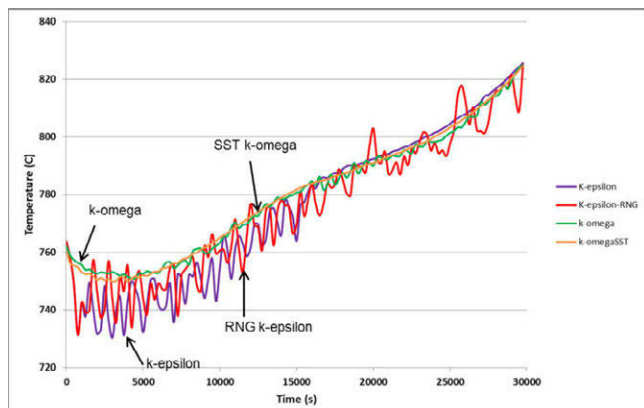


**Figure 7: Average flue gas temperatures for evaluated two equation turbulence models k-epsilon, RNG k-epsilon, k-omega and SST k-omega as denoted.**

The instability or wiggling of the burner flames for the k-epsilon and RNG k-epsilon models can be seen by the change in temperatures in the burner planes in a 60 second interval in Figure 8. This is less pronounced for the k-omega and SST k-omega models.

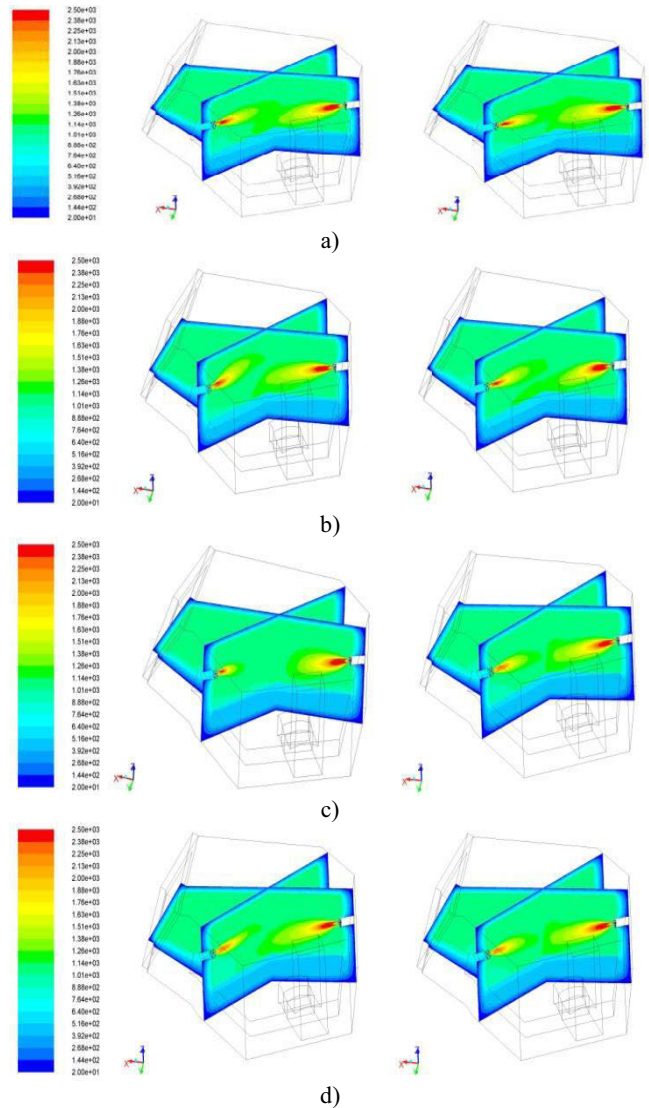


**Figure 8: Temperature contours in burner planes for turbulence models (a) k-epsilon (b) RNG k-epsilon (c) k-omega and (d) SST k-omega, at time 25019 s (left) and 60s later (right).**

#### Combustion models

For the evaluated 2-step reaction models in Figure 9, the Eddy Dissipation Concept model (EDC) gives lower heat of reactions than the Finite Rate/Eddy Dissipation model and the Eddy Dissipation model. The results from the two latter models coincide closely. This is due to the combustion being dominated by the mixing rate rather than the Arrhenius rate for the combustion.

The furnace temperatures in Figure 10 are lower for the Eddy Dissipation Concept combustion model due to the lower heat of reaction.

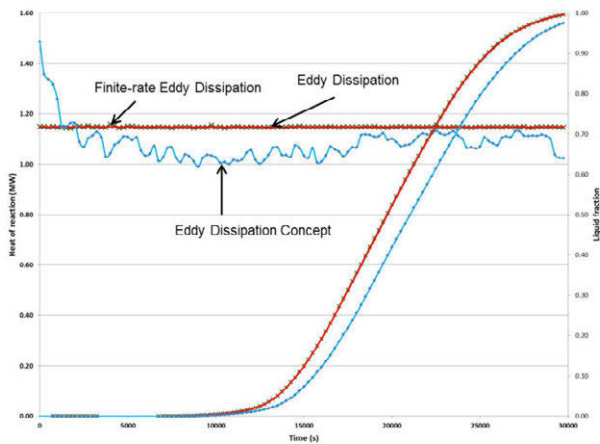


Figure 9: Heat of reaction and average liquid fraction for combustion models Finite-rate/eddy dissipation, Eddy Dissipation and Eddy Dissipation Concept.

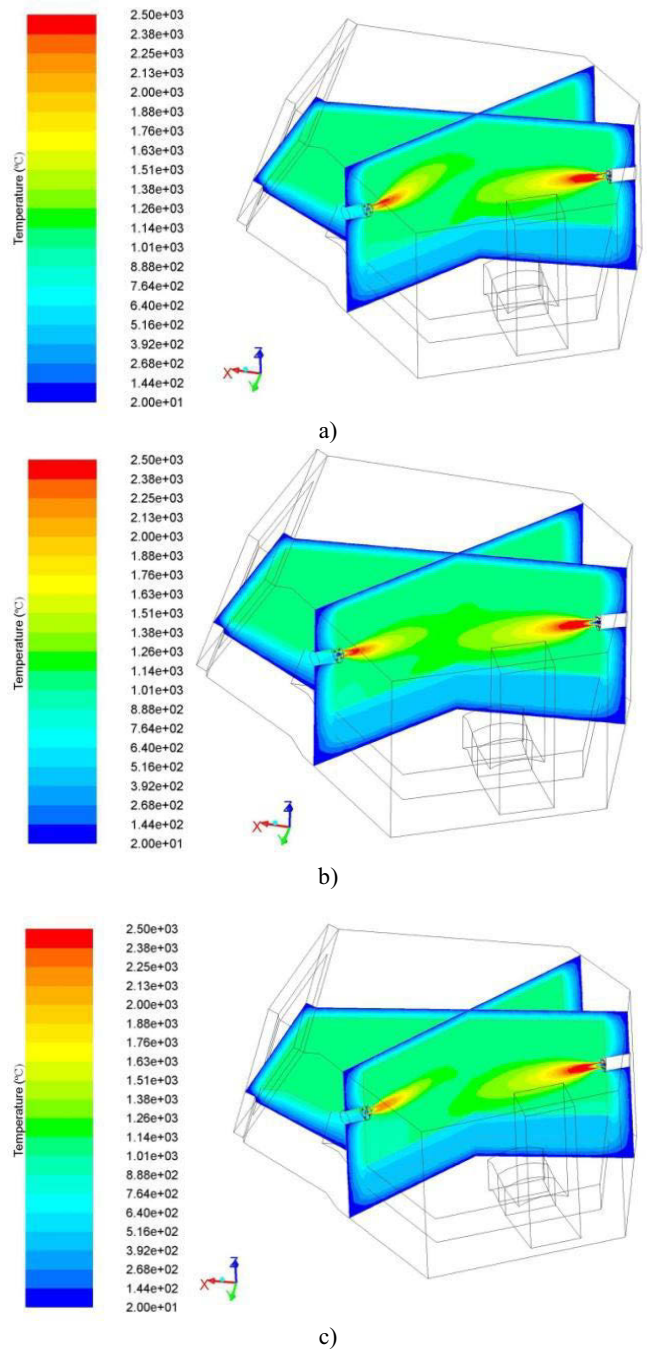
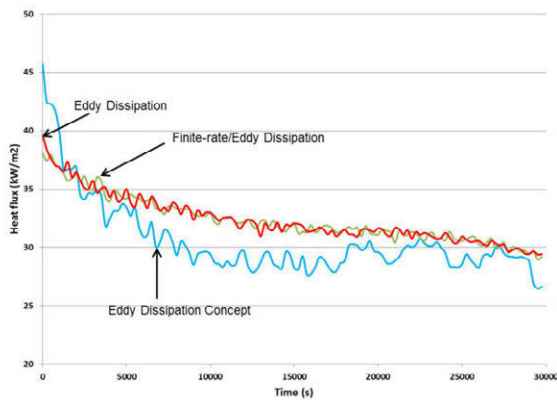


Figure 10: Furnace temperatures in burner planes at time 25019s for combustion case (a) Eddy Dissipation (b) Finite Rate/Eddy Dissipation (c) Eddy Dissipation Concept.

The surface heat flux into the melt pool surface in Figure 11 confirms the differences between the EDC model and the other two models. The change between the eddy dissipation concept model and the two other models shows that combustion is not only limited by the mixing rate but also by the chemical kinetics.



**Figure 11: Total melt surface heat flux for combustion models Finite-rate/eddy dissipation, Eddy Dissipation (red) and Eddy Dissipation Concept (light blue).**

### Conclusions

The numerical model was established to analyze the heat transfer conditions in a reverberatory melting furnace for oxy-fuel burner technology. The focus in the current work was investigating the difference between two equations turbulence models and two step reaction combustion models in this arrangement.

- The Eddy Dissipation Concept combustion model had clear differences compared to the other two evaluated combustion models. This resulted in lower furnace temperatures and slower heating of the metal.
- There were minor differences between the Eddy Dissipation model and the Finite Rate/Eddy Dissipation model as the combustion is dominated by the mixing rate and not the Arrhenius rate.
- The k-epsilon and RNG k-epsilon model showed fluctuations with time for the transient calculations which might indicate numerical stiffness.
- The k-omega and SST k-omega turbulence models gave more stable solutions for the furnace case.

### Acknowledgement

The authors would like to thank management at Hydro Aluminium Karmøy Rolling Mill for authorization and support in this project. Computing time at the Norwegian Metacenter for Computational Science (NOTUR) was appreciated for this work.

### References

1. **Andreas Buchholz, John Rødseth.** *Investigation of heat transfer conditions in a reverberatory melting furnace by numerical modeling.*: TMS Light Metals 2011, 1179-1184. p. 6.
2. **Jørgen Furu.** *An Experimental and Numerical Study of Heat Transfer in Aluminium Melting and Remelting Furnaces.* : Norwegian University of Science And Technology, 2013.
3. **Jørgen Furu et al.** *Numerical Modeling of Oxy-fuel and Air-fuel Burners for Aluminium Melting* : TMS Light Metals 2012, 1037-1042.
4. **D.C. Wilcox.** *Turbulence Modeling for CFD.* La Canada : DCW Industries, 1998.

5. **V.R. Voller, C.R. Swaminathan.** *General source-based method for solidification phase change.*: Numerical Heat Transfer, Part B (Fundamentals), 19 (2), (1991), 175-89.